Final: *Biosystems* **82:** 154-167, 2005

Studies of Intestinal Drug Transport Using an In Silico Epithelio-Mimetic Device

Yu Liu[1] and C. Anthony Hunt[1, 2 *]

[1]UCSF/UCB Joint Graduate Group in Bioengineering, University of California, Berkeley, CA, USA
[2]Biosystems Group, Department of Biopharmaceutical Sciences, University of California, San Francisco, CA, USA
*Corresponding author: hunt@itsa.ucsf.edu

Abstract

We report the development and use of a synthetic, discrete event, discrete space model that functions as an epithelio-mimetic device (EMD). It is intended to facilitate the study of intestinal transport of drug-like compounds. We represent passive paracellular and transcellular transport, carrier-mediated transport and active efflux using stand-alone components. Systematic verification of the EMD over a wide physiologically realistic range is essential before we can use it to address questions regarding the details of the interacting mechanisms that are believed to influence absorption. We report details of key verification experiments. We demonstrate that this device can generate behaviors similar to those observed in the *in vitro* Caco-2 transwell system. To do that we used a series of hypothetical drugs and we simulated behaviors for two clinically used drugs, alfentanil and digoxin. The results support the feasibility and practicability of the EMD as a tool to expand the experimental options for better understanding the biological processes involved in intestinal transport and absorption of compounds of interest.

Keywords

Intestinal drug transport, epithelial cells, systems biology, discrete event simulation

1. Introduction

Understanding the interplay among the mechanisms that influence the intestinal absorption of drugs in humans is critical to the successful development of orally administered drugs (Prentis et al. 1988). The *in vitro* model system based on Caco-2 cells, a human colon carcinoma epithelial cell line, is used widely in pharmaceutical research to study intestinal drug absorption and transport processes (Artursson et al. 1997). A variety of traditional mathematical models have been employed to help understand which mechanisms may be most important for different classes of compounds, and to make semi-quantitative predictions for new compounds or conditions (Parrott et al. 2002; Yu et al. 1999). These models have worked well in predicting the consequences of hypothesized mechanisms. They are not as useful, however, for testing hypotheses about interacting mechanisms or their details (Benet et al. 2004). Nor are they useful in linking those mechanisms to the expanding volume of biological data. Such hypotheses and linkages are typically tested using wetlab experiments. The model described here is an example of a class of models that can be built specifically to enable in silico testing of such hypotheses and exploring of linkages by conducting large numbers of distinct, easily automated experiments.

One of the best ways to learn about a phenomenon is to build a device that exhibits that behavior. To test hypotheses about actual mechanisms, we can construct a model of the posited mechanisms from component parts that map to counterparts in the referent, conduct experiments using the model, and show that the model behaves like the referent system under a sufficiently wide range of operating conditions. One approach is to develop synthetic, discrete event, discrete space, continuous time models (Ropella et al. 2005a; Ropella et al. 2005b) in which biomimetic, object-oriented software components can be plugged together and operated in ways that represent the hypothesized biological mechanisms within the referent wetlab system.

This is the first report of one example of this new class of in silico models. It is designed to study transport of drug-like compounds. The referent system is confluent monolayers of Caco-2 cells in a transwell device, and so we refer to our in silico model system as being an epithelio-mimetic device (EMD). This device is designed to generate biomimetic behaviors of epithelial cells and is constructed from software components that can map logically to biological counterparts at multiple levels of resolution. The first set of interacting mechanisms of interest includes passive paracellular and transcellular transport, carrier-mediated transport, and active efflux transport.

The paracellular route of absorption is taken primarily by small hydrophilic compounds while the transcellular route is taken by molecules that are sufficiently hydrophobic to partition into and then out of lipid bilayers. Hydrophilic molecules pass the cell monolayer via aqueous channels at tight junctions. Hydrophobic compounds mainly cross cell membranes using a process that involves breaking and reforming hydrogen bonds. For those orally administered compounds that mimic nutrients to some degree, carrier-mediated transport is either the only way, or an important way, to transverse the epithelial monolayer. There are two classes of transmembrane transporters. One consumes energy and can transport substrate against a concentration gradient. The other is not energy dependent and facilitates transport along the concentration gradient. All examples of both classes studied to date exhibit saturable kinetics.

Many different transporters are found in epithelial cells (Hidalgo et al. 1996; Tsuji et al. 1996). Some are found only on one side of the cell. Others can be found in both locations. Some work in both directions (e.g., PepT1 in the apical (A) membrane transports drugs in and out), whereas others work in only one direction (e.g., MRP-1 in the basolateral (B) membrane only transports compounds out, i.e., A to B). P-glycoprotein (P-gp, the MDR-1 gene product) is present in the apical membrane of enterocytes and many other cell types. It is a promiscuous transporter for xenobiotic removal. In the intestine, it actively transports a variety of compounds, including many drugs and their metabolites, out of intestinal epithelial cells. It functions as an efflux pump and it is believed to help protect the individual against absorption of potentially toxic substances.

Our goal is to have useful, extensible EMDs suitable for assessment of interacting drug metabolism and transport-related mechanisms. We envision a variety of scientific uses for such devices. All, however, require that EMDs function as objects for experimentation, where some of the in silico experiments are designed to explore and address mechanistic questions and hypotheses that are difficult or impossible to address using either traditional wetlab or mathematical modeling methods. The purpose of this report is to demonstrate that we can build an EMD that is a practicable device for experimentation, and, most importantly, to report on experiments that help verify that the device can function as intended, and that it generates behaviors similar to those observed in experiments using the *in vitro* Caco-2 transwell system. Systematic verification is an essential first step before beginning to explore mechanistic questions of interest.

2. Inductive vs. Synthetic Models

The models mainly used in biomedical research fall into two broad categories: constructed wetlab models and induced mathematical models. Wetlab models, including *in vivo, in situ,* and *in vitro* models, are the mainstay of biomedical research (cell cultures, isolated, perfused organs and tissues, etc.). They are synthetic models where some of the building blocks are laboratory items and others are living parts. The Caco-2 transwell system is an example of such synthetic models. There is a huge gap between the experimental wetlab models and traditional computational models. This gap sits on a continuum between the two extremes of experiment and theory. To make progress toward understanding biological complexity we need to bridge this gap, and to do that we need new methods. From these new methods will come new classes of models that make computational biology more experimental and wetlab research more computational. The EMDs are intended to make progress narrowing that gap.

The inductive method (Steels et al. 1995) for creating mathematical models dominates the biomedical literature. Examples include the oral drug absorption model (Grass 1997) and the more elaborate,

physiologically based toxicokinetic model (Andersen 2003). These models are usually built by analyzing data, creating a mapping between the envisioned structure of the experimental system and components of the data, and then representing those data components with mathematical equations. The equations are then implemented, executed, and validated against the data. This modeling method relies heavily on mental knowledge combined with induction. It stays very close to the data and, when successful, provides models that extrapolate beyond the original data, making them usable for prediction. However, these equation-based models lack particulars. The detail that is washed away when an equation is induced is where all the heuristic value lies. That detail describes the mechanism by which the data were generated, whereas the mathematics only describes the abstracted properties of the data.

To better understand how a mammalian system such as the intestine, or even a much simpler *in vitro* model system such as the cultured cells in a transwell device, generates a seemingly endless variety of robust and fragile behaviors, we need to construct models that can exhibit some of those behaviors. The constructive or "synthetic" method (Steels et al. 1995; Zeigler 1990) consists of proposing and constructing building blocks that can be assembled to create an artificial system that functions in the real world. One can look inside such a system and observe the components and how they interact as the system operates. With the advance of object-oriented (OO) programming it has become feasible to build such synthetic models computationally (Zeigler 1990). It has also become easier to construct large system models where the modular components are not parts of a mechanism, but are themselves inductive models. The sophisticated physiologically based models constructed as part of the Physiome Project[1] are examples of the latter. With the most recent progress in OO programming has come the ability to actually build, in silico, a functioning model of the mechanism of which an inductive model is an abstraction. That is what we have done here.

An essential difference between inductive models and synthetic models lies in the fact that the inductive method explicitly uses the observed phenomena (the data) as its input whereas the synthetic method starts with proposed building blocks and relations between them (Ropella et al. 2005b). Consider a mapping from the space of generator mechanisms to the space of phenomena. The inductive method starts with the phenomena and works backward to the generators in an attempt to discover an *inverse* mapping from range to domain. The synthetic method, in contrast, works *forward* from domain to range. Its constraints and criteria sit primarily in the domain. It should be clear that neither method is superior. An inductive model will provide a better fit to the data and a better extrapolation of that data if the experimental conditions are kept the same. The synthetic model will provide a hypothesis for the "machine" that is believed to generate the data. An inductive model allows one to make claims *about the data*. The synthetic model allows one to make claims *about the mechanism.* Synthetic modeling requires knowledge of the function of the referent, of plausible mechanisms for that function, and of relevant observables by which the analog and the referent will be measured. For the in silico models described here, considerable histological, physiological, experimental, and operational knowledge is already available. That is a key reason for selecting the above-mentioned *in vitro* model as a starting place. Because the effort required to build a model of the EMD type is nontrivial, it is essential that the operation of the device and its modular components be verified over a wide, physiologically realistic range before undertaking exploratory experimentation. This report also presents results of experiments designed to provide that verification.

3. Methods

3.1 EMD Structure and Design

The EMD described below is intended to mimic essential aspects of the Caco-2 *in vitro* cell culture system that, in turn, is a biological model built to represent the mature epithelia lining the villi of the small intestine, and enable study of the permeability of that barrier. Caco-2 cells are typically grown to confluence on the microporous membrane insert of the transwell diffusion system (Fig. 1). Thereafter the

[1] Physiome Project: http://www.physiome.org/

system is used as an experimental model, primarily in drug transport studies. The chamber of the transwell insert represents the apical side, the intestinal lumen. The well, into which the insert fits, represents the basolateral side of villi adjacent to the intestinal capillaries. The structure of the EMD mimics these essential features along with the permeable membranes of the Caco-2 cell monolayer and aspects of intracellular biochemical systems.

The EMD represents a vertical column section through the entire transwell system with an arbitrary width. This section is sliced virtually into five stacked segments. Each slice is subdivided into 10,000 elements (100 x 100 2D grids). New spaces can be added by plugging in new grids. That can be done without interfering with the function of the existing spaces or having to re-engineer the EMD. The horizontal resolution can be increased in two ways: increase the number of grid subdivisions (e.g., from 100^2 to 200^2), or decrease the width of the virtual column section to which the EMD maps. *G1* represents the apical lumen compartment and a portion of the fluid in the transwell cell culture insert. *G2* represents apical membranes of cells and the junctions between them viewed from the apical side. *G3* represents the intracellular space. *G4* represents basolateral membranes and the junctions between cells viewed from the basolateral side. Within *G2* and *G4*, a parameter controls the prevalence of tight junctions between cells. Currently, at the start of each in silico experiment, 0.1% of grid points in each of these two spaces are chosen randomly and assigned to be junctions; the remaining 99.9% represent cell membrane (Artursson et al. 2001). *G5* represents a portion of the basolateral compartment and the fluid in the cell culture well. These spaces accommodate the other components of the system. Drug molecules are represented as objects[2] that can move within and among spaces. A typical DRUG[3] object represents more than one drug molecule. The transporters embedded in the cell membranes are modeled as immobile objects. They are assigned randomly to the *G2* and/or *G4* spaces. Because there may be several transporters within the area of cell membrane represented by one grid point, each TRANSPORTER object may represent more than one transporter. Objects representing transporters can interact with mobile DRUGS in their immediate vicinity. Additional objects or agents, e.g., metabolic enzymes, networks that control the level of expression of transporters, or other cellular components, can be specified and added as needed.

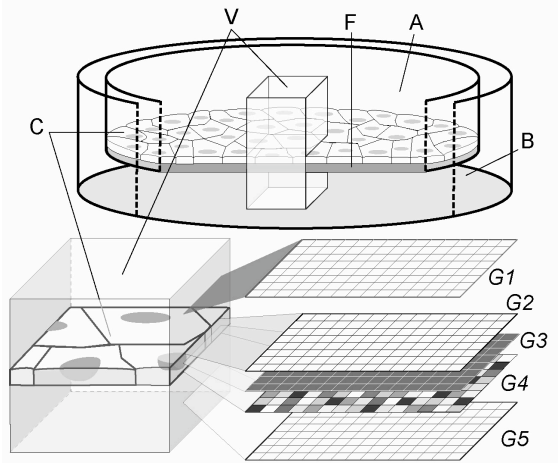

Figure 1. *In vitro* and in silico experimental devices to study intestinal drug transport. Caco-2 *in vitro* transwell system: A: apical compartment; B: basolateral compartment; C: epithelial cell monolayer; F: filter; V: a vertical column section through the transwell system. Epithelio-mimetic device (EMD): *G1–G5*: 2D grid spaces representing the indicated components of the referent *in vitro* transwell system.

[2] Objects within the EMD can be either simple, passive objects or agents. The latter are capable of interacting with their environment and scheduling their own activities.

[3] When referring to the in silico counterpart of a compound, a drug, a biological component, such as "membrane," or a cell component such as "transporter," we use SMALL CAPS.

The different shading of the *G4* grid locations illustrates that individual grid locations in any of the five spaces can have different properties (see the text for additional detail).

The in silico device is intended to be exercised and measured during the course of experimentation in the same way as its referent *in vitro* experimental system. Consequently, within the computational framework (Fig. 2) one needs an agent to manage the in silico experiments. In the EMD we refer to that agent as the *Experiment Agent*. It is the in silico counterpart to the researcher conducting wetlab experiments. The *Data Model* holds data taken from the referent system and the *Reference Model* is an existing mathematical model that has been widely accepted to represent some system behaviors. In each in silico experiment, the *Experiment Agent* reads inputs from the *Parameter Manager* and transfers that information to the experimental device, the EMD. The simulation results are collected in the *Data Management Module* and processed in the *Statistical Observer Module*. We built the EMD framework using the JAVA layer of the Swarm platform (Gilbert et al. 2002).

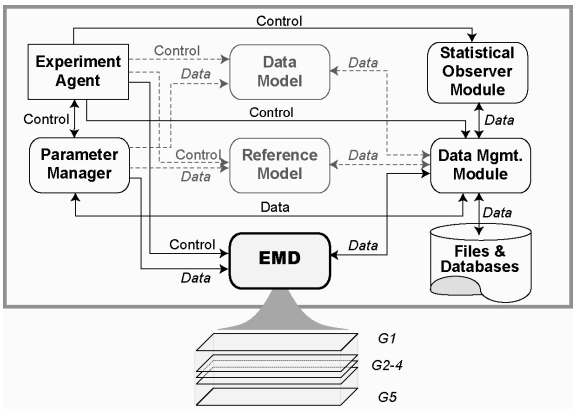

Figure 2. The Computational framework of the EMD. Additional detail is provided in the text. The *Experiment Agent* manages the in silico experiments. It controls all of the other components in the framework.

3.2 Passive Transport in the EMD

Within each grid space, at any step, a free DRUG can move to an adjacent, less-crowded location within that grid space. Such movement is governed by a biased random walk. Transition of a DRUG from one space to another is governed by its location (e.g., being at a tight junction or near a lipoid membrane structure), its assigned physicochemical properties, and environmental conditions, including the concentration gradient across the simulated cell monolayer, pH, etc. The simulation of permeation during experiments takes into account the influence of the concentration gradient along with three interrelated physicochemical properties: lipophilicity, degree of ionization (calculated from pH and pK_a), and molecular size. We assume that small (≤ 200 Dalton) hydrophilic compounds having partition coefficients (P) less than 2 can pass through cell monolayers only by passive paracellular transport via aqueous pores. For those more hydrophobic compounds no larger than 1000 Daltons, passive transcellular transport is a function of the unionized fraction. We assume that transport increases with increasing log$P$ values (increasing lipophilicity) up to 2.5~3.5, and declines thereafter (Camenisch et al. 1998a; Wils et al. 1994). Molecular weight (MW) is used as the simplified molecular size descriptor and is related to the in silico diffusion coefficient (D_{EMD}): $D_{EMD} \propto 1/(\mathrm{MW})^n$. In these studies we assume n = 1 in the bilayer and 0.6 elsewhere (Walter et al. 1986; Xiang et al. 1993). We also assume that entering the bilayer from an aqueous space is the rate-limiting step, influenced by the above factors, whereas exiting the bilayer is fast with a 50% chance.

3.3 Carrier-Mediated Transport and Efflux

In our current EMD, we have implemented a generic class called TRANSPORTER, which can be located in either membrane space and can transport in either or both directions. TRANSPORTER is designed to function as diagramed in Fig. 3. If a DRUG substrate is located at the grid point adjacent to the free binding site, binding can occur with a probability that depends on their affinity. Binding triggers a conformational change (TRANSPORTER's "door" opens) so that the DRUG can cross from one side of the bilayer to the other. At the next time step TRANSPORTER releases the DRUG and then reverts to its free state. P-gp is modeled as a distinct type of TRANSPORT called PGP. In this study PGP is confined to *G2* and is parameterized to only transport DRUGS out of the simulated cell interior to *G1*.

3.4 Design of In Silico Experiments and Data Analysis

In Table 1 the parameters of the EMD are grouped into three categories: 1) the in silico transwell system, including CELL and TRANSPORTER characteristics; 2) the physicochemical and biochemical properties assigned to DRUGS; and 3) the in silico experimental conditions. The in silico transwell system is designed to study and document DRUG transport from either direction. When *G1* is designated as the donor compartment, the EMD simulates apical-to-basolateral (A to B) transport; when *G5* is designated as the donor compartment, the EMD simulates B to A transport. The simulated concentration-time profile is recorded at each time step for all five spaces. Additional observations of interest are also recorded for use in subsequent analyses. Examples include the number of DRUGS passing through CELL-CELL junctions and the number of occupied TRANSPORTERS. In this study, in silico experiments are run under a sink condition, i.e., until ≤ 10% of DRUGS have transported from the donor space (*G1* or *G5*) to the receiver space (*G5* or *G1*). The initial flux rates are calculated by dividing the number of DRUGS in the receiver space by elapsed time steps. We calculate in silico apparent permeation coefficient: $P_{EMD} = (dQ/ds)/(a \times c_0)$, where dQ/ds is the initial flux rate, a is the area of the first MEMBRANE space contacted (either G2 or G4, which are the same in this report), and c_0 is the initial concentration (dose) of DRUGS in *G1* or *G5* at time step 0.

Because of the stochastic nature of the EMD simulations, repeated measurements of a behavior of interest, such as flux rates, will differ between trails. During exploratory modeling, we prefer to make decisions or draw conclusions about mechanistic issues using relatively small sample sizes, e.g., results from 5-10 Monte Carlo simulations. To build confidence that central limit theorem results can apply to the EMD behaviors, most of the experimental results reported here are based on at least 30-50 trials.

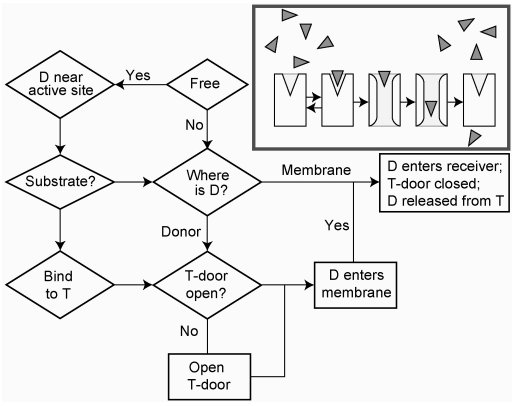

Figure 3. A flowchart diagram for the carrier-mediated transport component. D: a DRUG object; T: a TRANSPORTER object. The algorithm is designed according to the schematic in the insert. Triangle: DRUG; notched and open white boxes: different TRANSPORTER states. Binding between T and D is probabilistic and is controlled by the simulation parameter *transSoluteAffinity*.

Table 1. Parameters of the EMD

Category	Name	Description	Values
In silico transwell system	*worldXSize* *worldYSize*	The X x Y dimension of *G1 – G5*	100 x 100
	tightJunctions	Tight junction area as % MEMBRANE space area	0.1
	minTransporters	Minimum density of TRANSPORTER	10
	maxTransporters	Maximum density of TRANSPORTER	80
	apiBasoRatio	TRANSPORTER density ratio (A to B)	≥ 1
	minPgps	Minimum PGP density	10
	maxPgps	Maximum PGP density	30
	cellular_pH	Simulated *G3* (CYTOPLASM) pH	7.2 ~ 7.4
Physicochemical and biochemical properties of DRUGS	*molecularWeight*	MW (molecular weight)	100 ~ 1200
	acid	DRUG is a weak acid or weak base	T or F
	pK$_a$	DRUG's pK$_a$	6.5 or 13.5
	logP	Logarithm of partition coefficient	-2 ~ 4
	ionDiffusion	Permeation due to ionized form of DRUG (%)	0 ~ 1
	substrateOfTransporter	DRUG is a substrate of TRANSPORTER or not	T or F
	transSoluteAffinity	DRUG–TRANSPORTER binding affinity	0 ~ 0.5
	substrateOfPgp	DRUG is a substrate of PGP or not	T or F
	pgpSoluteAffinity	DRUG–PGP binding affinity	0 ~ 0.75
Exp. Condition	*numSolutes*	Initial concentration in donor compartment	500 ~ 8000
	gIpH	Simulated *G1* (apical) pH	5 ~ 8
	gVpH	Simulated *G5* (basolateral) pH	7.4
	a2bDirection	Donor is *G1* or *G5*	T or F

4. Results

4.1 Factors Influencing Passive Transport

When an *in vitro* transwell system is functioning properly, the passive transport of compounds studied is directly proportional to their concentrations in the donor compartment over a wide concentration range. We expect simulated passive transport in the EMD to behave similarly. To verify that this is the case for both passive transcellular and paracellular transport we evaluated permeability in the EMD for two hypothetical weak basic DRUGS, both having pK$_a$ = 6.5 and MW = 150. DRUG I is hydrophobic with log*P* = 2; DRUG II is hydrophilic with log*P* = 0.2. The in silico pH of *G1, G3,* and *G5* was fixed at 7.4, unless otherwise noted. At that pH both DRUGS are 11.18% ionized. Experiments were conducted to measure initial flux rates for a wide range of initial concentrations. The results for both transport routes are presented in Fig. 4. Higher initial concentrations resulted in proportionally higher rates of permeation for both DRUG I and II, as expected. At each concentration, transcellular transport is faster than paracellular transport due to the 1000-fold smaller available surface area of the paracellular route.

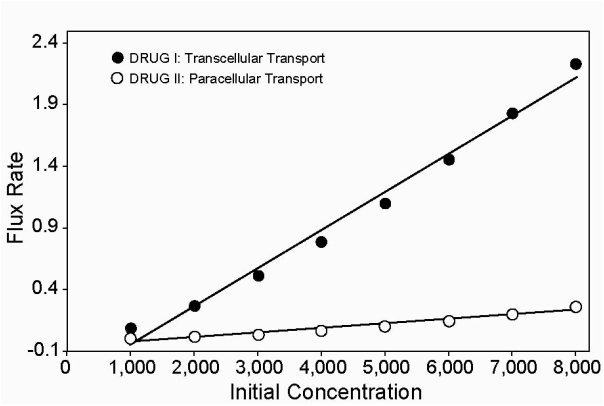

Figure 4. A scatter plot of in silico experimental results. The flux rate across in silico monolayers is plotted vs. the amount of DRUG added to the donor space. The data shown are the means of 50 and 30 Monte Carlo simulations respectively for each initial concentration of two hypothetical drugs: hydrophobic DRUG I and hydrophilic DRUG II; R^2 values of the two linear regressions are 0.99 and 0.96 respectively. Reasonable linear relationships are observed when the initial amounts added are between 2000 and 7000 DRUG objects, the current range of interest.

A modification of Fick's law, $dQ/dt = \Delta C\ (D \times P \times A)/\Delta x$, has been used successfully to represent passive transport across cell membranes (Avdeef 2001), where dQ/dt is the flux or permeation rate, A is the area of membrane through which solutes pass, ΔC is the concentration gradient, and Δx is the thickness of membrane. From this equation, we can see that flux is expected to be positively correlated with both partition coefficient P and diffusion coefficient D, as well as being proportional to the initial concentration. To verify that those relationships can be observed in the EMD, we did a series of A to B transport experiments to examine the influence of simulated lipophilicity and molecular size on simulated passive transport. Experiments were conducted in the absence of transporters using identical doses (2000 DRUGS) of five sets of hypothetical DRUGS having MW values of 100, 150, 300, 500, and 700, and log$P$ values ranging from very hydrophilic (log$P$ = – 2) to very hydrophobic (log$P$ = 4). In each case the in silico experimental results were used to calculate an in silico permeability. Those values were then plotted vs. partition coefficient. For DRUGS with log$P$ values less than 3.5, sigmoidal curves were observed (Fig. 5) that have shapes similar to those reported in Camenisch et al. (1998a; 1998b). For DRUGS with larger MW values, the curves were shifted to lower permeabilities, as expected. Four patterns were observed, consistent with those observed in Caco-2 transwell system (Camenisch et al. 1996). DRUGS with small log$P$ values (≤ 0) were too hydrophilic to significantly cross MEMBRANES unaided, so the passive paracellular pathway dominated for six DRUGS having MW ≤ 150. For more hydrophobic DRUGS, paracellular transport quickly became negligible, and transcellular permeability increased with increasing lipophilicity. For those DRUGS having log$P$ between 2.5 and 3.5, the expected permeability plateaus were reached. For highly hydrophobic DRUGS (log$P$ > 3.5), permeability decreased with further increases in lipophilicity.

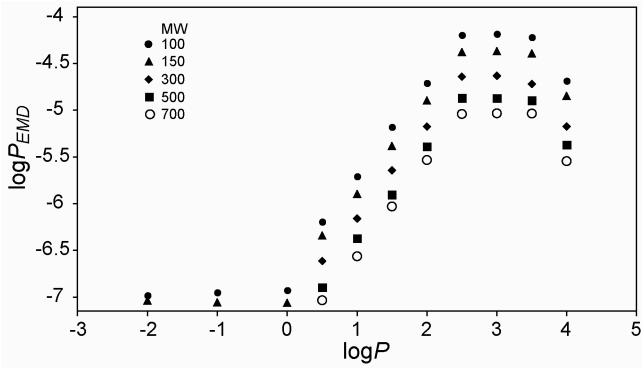

Figure 5. A log-log plot of in silico experimental results. Simulated initial permeability is plotted as a function of lipophilicity for five sets of drugs having the indicated molecular weights.

Each portion of the human gastrointestinal tract typically experiences a different range of pH. For example, the interior of the major absorptive part of small intestine, the duodenum, typically has pH values in the range of 6.0~6.5, which favors absorption of weak base drugs. Consequently, it is important that we be able to explore simulated transport under a variety of pH conditions. We explored pH-dependent passive transport in the EMD using a simulation of a potent opioid analgesic drug, alfentanil: MW = 416, log*P* = 2.16, and pK_a = 6.5 (weak base). At pH = 5.0 alfentanil is mostly ionized; at pH = 8.0 it is mostly unionized. We conducted multiple Monte Carlo experiments at each of nine different *G1* pH values ranging from 5.0 to 8.0. The pH in *G3* was kept constant at 7.4. The results in Fig. 6A indicate a linear relationship between the in silico permeability and unionized fraction. We observed a nonlinear relationship between the in silico permeability and the pH value in the donor space (Fig. 6B). Both sets of experimental results are quite similar to the reported *in vitro* results for alfentanil permeability (Palm et al. 1999).

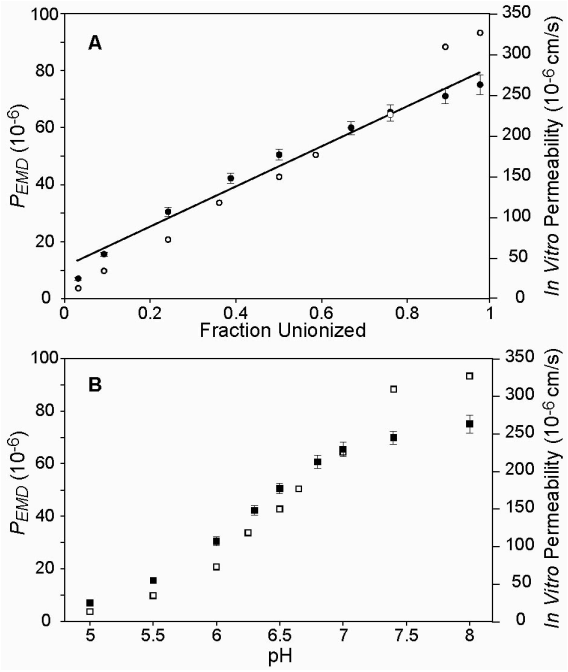

Figure 6. A comparison of experimental results from in silico and *in vitro* model systems. Open symbols: *in vitro* measures of alfentanil permeability; the values (right axis) are the means reported in Palm et al. (1999) for each of nine transwell apical compartment pH values. Closed symbols: in silico measures of the permeability of ALFENTANIL in the EMD. The values (left axis) are mean ± S.D. from 50 Monte Carlo simulations for each of nine *G1* pH values. A: permeability as a function of the

unionized fraction in the apical compartment or the *G1* space. The regression line for the in silico results ($R^2 = 0.97$) is shown. B: permeability as a function of the pH in the apical compartment or the *G1* space.

4.2 Modeling Saturable Kinetics for a Protein Mediated Process in the EMD

Within the EMD, at the software level, components such as TRANSPORTER, PGP, etc., are intended to function as modules that can be added or removed as needed, and even used in different biomimetic models simulating different aspects of biology. As modules, their behavior and function should be independently verified. Thereafter, a test can be done to verify expected function after the module is inserted into the EMD (or any other model).

Both the carrier-mediated transport module and the efflux module are designed to simulate an interaction between PROTEINS and DRUGS that follows simple Michaelis-Menten kinetics. The actual units of variables and parameters in a typical Michaelis-Menten model are not the same as those governing the discrete event, continuous time process. We can, however, verify that the latter can serve as a model for the former by demonstrating that the two models generate similar output under similar operating conditions. We carried out such comparisons over a wide range of variable and parameter values. Examples are provided in Fig. 7. We analyzed the kinetics at a low (25) and a high (150) ratio of DRUGS to PROTEINS. In the Michaelis-Menten model the magnitude of this ratio controls the shape of the time series. If the concentration of the DRUG relative to the PROTEIN is relatively small, then there is always free PROTEIN and the time course of product formation exhibits first-order kinetics. If the relative concentration is large, then there will be less free PROTEIN and the time course of product formation will begin to exhibit zero-order kinetics. In Fig. 7, the left pair of graphs shows the continuous concentration-time output from the Michaelis-Menten model implemented in Matlab. The right pair of graphs shows the output of the discrete event model implemented in the EMD. Each step in the EMD simulation corresponded to approximately 0.033 time unit in the mathematical model. The kinetic profile for both sets of data, at a small and large ratio of DRUGS to PROTEINS, exhibited similar patterns.

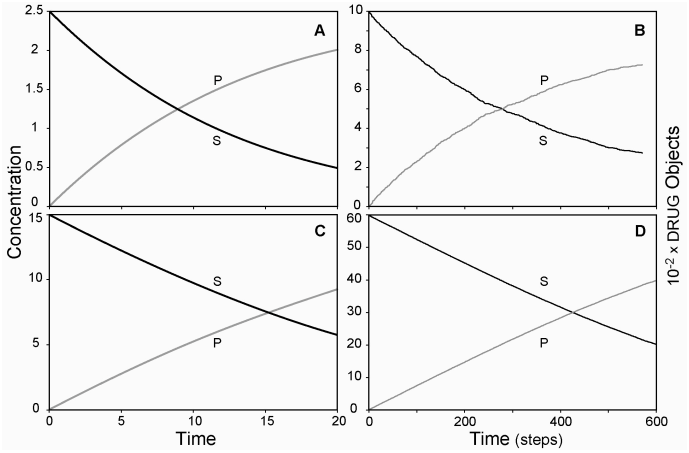

Figure 7. Simulated results from the classical Michaelis-Menten mechanism are compared for two model types. The mechanism: $E + S \underset{k_{-1}}{\overset{k_1}{\longleftrightarrow}} ES \underset{k_{-2}}{\overset{k_2}{\longleftrightarrow}} P + E$; S is substrate, E is protein (an enzyme), ES is the intermediate complex, and P is product. A and C: simulated output from the equation form (ODE) of the Michaelis-Menten model implemented in Matlab. B and C: the above mechanism implemented in the EMD (discrete event, discrete space, continuous time). A and B: the S/E ratio = 25. C and D: the S/E ratio = 150. In the ODE model: $k_1 = 1$, $k_{-1} = 1$, $k_2 = 10$, and $k_{-2} = 0.01$. The EMD simulations used 40 E, each having the highest binding probability (1.0) with S.

4.3 Carrier-Mediated Transport

For each in silico experiment the total number of TRANSPORTERS was determined by a random draw from a uniform distribution that had limits specified by the parameters *minTransporters* and *maxTransporters*. A portion of these objects was then assigned to the apical (*G2*) or basolateral (*G4*) membrane spaces according to the parameter *apiBasoRatio*, which specifies the density ratio of transporters in these two membranes. That ratio controls DRUG transport kinetics. Note that in studies of A to B carrier-mediated transport under the sink condition there is always more DRUG in *G1* than in *G3*. Therefore, there will be more substrate for the TRANSPORTER embedded in *G2* than in *G4*. For this reason, we studied the disappearance rate of DRUG III (MW = 1200 Daltons) from *G1* space in A to B transport experiments. We limited the number of TRANSPORTERS in *G2* to 10 to 80, and did 100 Monte Carlo simulations. In each simulation, 2000 DRUGS were added to the *G1* space at time zero and their *transSoluteAffinity* was set to 0.5. The initial transport rates were plotted against the number of TRANSPORTERS in *G2*. A linear relationship exhibiting a large correlation was observed (Fig. 8A).

We also did a series of similar experiments by changing the initial dose added to *G1* while limiting the number of TRANSPORTERS in *G2* to be either 15 or 27. The transport rate increased slowly with higher drug dose and had a tendency to reach a maximum. We used a nonlinear least square algorithm to fit the simulated transport rate vs. dose data to a traditional Michaelis-Menten model and the results are shown in Fig. 8B. For the simulations with 27 TRANSPORTERS in *G2*, the fitted V_{max} = 9.17 ± 0.08, and K_m = 7019 ± 107; for the simulations with 15 TRANSPORTERS in *G2*, the fitted V_{max} = 5.14 ± 0.05, and K_m = 7113 ± 121. The binding affinity between a TRANSPORTER and a DRUG corresponds to K_m in the Michaelis-Menten model. The value of the maximum transport rate depends on both the number of TRANSPORTERS and their affinity for DRUG, as expected. Taken together, the results verify that the functioning of the TRANSPORTER module mimics simple Michaelis-Menten kinetics over the conditions studied.

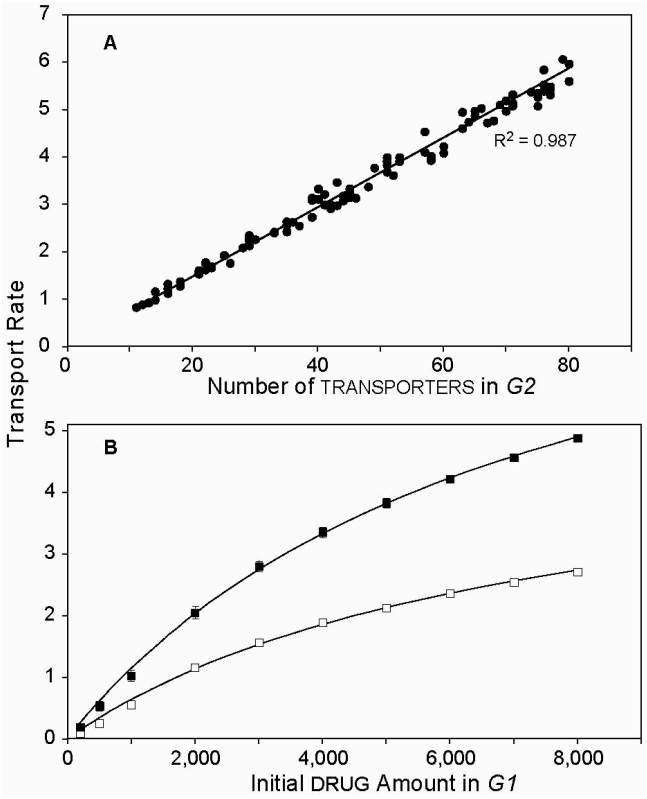

Figure 8. Scatter plots of the disappearance rate of DRUG III from *G1* in A to B transport experiments. DRUG III's MW is 1200 Dalton, well above the limit for passive transport. A: Results show a linear

relationship between DRUG disappearance rate and the number of TRANSPORTER objects in *G2*. For each of 100 Monte Carlo simulations, 2000 DRUGS were randomly placed in *G1* at $t = 0$. For each experiment, the number of TRANSPORTERS in *G2* was determined by a random draw from a uniform distribution having a minimum of 10 and a maximum of 80. The fit shown is a straight line with an intercept of zero. B: Results show a saturable relationship between the disappearance rate and the number of DRUGS initially placed in *G1*. Solid squares: 27 *G2* TRANSPORTERS; open squares: 15 *G2* TRANSPORTERS. The data are shown as mean ± S.D. from 50 Monte Carlo simulations. In both cases the solid curve is the result of fitting the Michaelis-Menten ODE model to the data using a nonlinear least square algorithm.

4.4 Efflux Changes Drug Transport

To test if a higher affinity and/or a larger number of PGP objects in the *G2* space can change the transport activity across the in silico monolayer, we created two "analogs" of DRUG I, DI.1 and DI.2, which are exclusive substrates of PGP. They have *pgpSoluteAffinity* of 0.5 and 0.75, respectively. As a non-substrate of PGP, DRUG I did not, of course, demonstrate any significant difference between A to B and B to A transport. For DI.1 and DI.2 net transport across the monolayer in the B to A direction increased relative to DRUG I, whereas that in the A to B direction decreased. The difference in transport in the two directions was statistically significant (Fig. 9)[4], verifying that the function of PGP module mimics the behavior of apical membrane efflux transporters *in vitro*. Moreover, having a higher PGP affinity and/or density resulted in more dramatic changes in both directions.

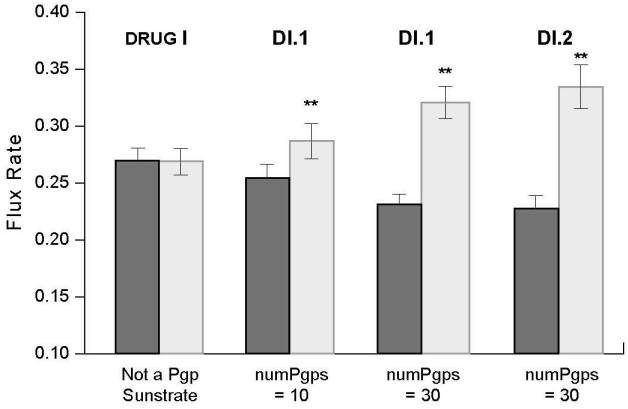

Figure 9. A bar graph showing the influence of efflux transport on the simulated flux rates of three hypothetical DRUGS. Their physicochemical properties are the same (DRUG I in the text). DRUG binding affinities for PGP are 0 for DRUG I, 0.5 for DI.1, and 0.75 for DI.2. The number of PGP in *G2* was 10 or 30. 2000 DRUGS were initially placed in the donor space. Solid bars: simulated A to B transport. Shaded bars: simulated B to A transport. The data are shown as mean ± S.D. from 30 Monte Carlo simulations. **: Significantly different from A to B transport for that condition (Welch test, $p < 0.01$).

Digoxin, a weak acid ($pK_a = 13.5$) cardiac drug, is an exclusive substrate of P-gp in human enterocytes. Because of its relatively large MW (781 Daltons) and low log*P* (1.14), its passive transport is slow. That, combined with active efflux transport from the intracellular space back to the intestinal lumen, dramatically retards its absorption. We simulated digoxin transport in the EMD and compared the time-course of the in silico experiments with that observed in the *in vitro* experiments using CYP3A4-transfected Caco-2 cells (Cummins et al. 2001). Digoxin's physicochemical properties were assigned to DIGOXIN in an EMD having a PGP density ranging from 10 to 30. We set the PGP–DIGOXIN affinity to be 0.5, and ran 30 15,000-time-step Monte Carlo simulations for each transport direction with a dose of 4000 DIGOXIN objects. Figure 10 shows the simulated transepithelial flux of DIGOXIN across in silico

[4] We used the Welch modified two-sample t-test instead of the standard t-test because we assumed that the variances of the A to B transport data and the B to A transport data were not necessarily equal.

monolayers together with the *in vitro* data taken from Cummins et al. (2001). Transport in the B to A direction greatly exceeded that in the A to B direction. This difference in directional transport is more than those seen for DI.1 and DI.2 (Fig. 9) because the physicochemical properties of DI.1 and DI.2 favor much faster passive transport and thus shorter intracellular residency time. Having relatively fast passive transport dilutes the influence of efflux transport. When the in silico results were mapped to the *in vitro* results, as shown in Fig. 10, we saw that each simulation step corresponded to approximately 0.56 seconds in the *in vitro* experiments. The efflux ratio (the [B to A]/[A to B] flux ratio) was about eight in this EMD and was about five in the *in vitro* system. The higher in silico efflux ratio can be decreased to about five by either decreasing the PGP density in the system or decreasing the binding affinity between DIGOXIN and PGP. In future experiments, where model validation has become an objective, PGP density and PGP–DIGOXIN affinity will likely be among the parameters adjusted.

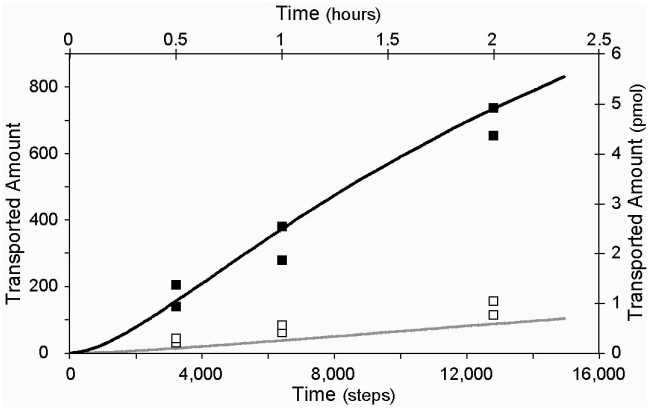

Figure 10. Time series plots show the amount of digoxin and its in silico analog transported in both directions in an *in vitro* transwell system and in an EMD. *In vitro* experiments: the filled and open squares (top and right axes) are the upper and lower mean values from a set of four different *in vitro* experiments that measured the initial flux of digoxin (30 nM) across CYP3A4-transfected Caco-2 cells. The data are from Cummins et al. (2001). Filled squares: B to A transport. Open squares: A to B transport. The [B to A]/[A to B] efflux ratio is about five. In silico experiments: the two curves (bottom and left axes) are the mean values at each time step of 30 Monte Carlo experiments that measured the flux of DIGOXIN for B to A transport (dark line) and A to B transport (gray line), respectively. The [B to A]/[A to B] efflux ratio is about eight.

5. Discussion

Our goal is to have useful, extensible EMDs that are suitable for experimentation, where functional components can be plugged together to study and better understand the details of the multiple interacting mechanisms that influence drug absorption. We have developed and successfully tested a synthetic EMD that has flexible, discrete event, discrete space, and continuous time features. The assembled biomimetic components exhibit mechanistic details that are typically abstracted away in the inductive models. We have demonstrated that the behaviors of the EMD successfully represent aspects of three drug transport processes within the *in vitro* Caco-2 system: passive, carrier-mediated, and efflux transport. The verification experiments have focused on patterns of transport under the sink condition rather than on the generation of predictions for specific compounds, in part because pattern identification and pattern matching are essential parts of our method.

Experimentation with synthetic models is expected to work synergistically with wetlab experiments to provide researchers with a richer set of options to select among the mechanisms that are hypothesized to cause observed transport phenomena. The EMD also provides modular methods for representing the spatial organization of mechanistic details. That spatial organization is an important feature of biological reality that is too often missing from traditional inductive models. This new class of models makes possible the extension of experimental biology into the in silico computational domain. That extension

represents important progress in bridging the gap between the wetlab models and traditional computational models.

Currently, the entire intracellular space is represented by only one 2D grid (*G3*). When required, relevant intracellular objects can be assigned randomly within that space. That low-resolution representation is adequate to account for the simple transport phenomena being considered here. A more spatially complicated mechanism that, for example, may need consideration of the transcellular arrangement of objects between the basolateral and apical sides of the cell, will require enabling more space. The problem can be solved by treating *G3*, and all the functionality that it contains, as a modular submodel within the EMD, which can be unplugged and replaced with another submodel designed to mesh properly with the rest of the EMD. The replacement module can be one that has a higher resolution. A requirement will be that each new module can generate the same behaviors as *G3*, relative to the rest of the EMD, for identical EMD parameter settings. Of course, because of the additional resolution, the new submodel is expected to enable the EMD to generate behaviors that are beyond those of the current EMD implementation. For example, one can use a submodel that is simply an ordered set of n ($n > 1$) 2D grids. If having additional spatial regions in a submodel is more important, in order, for example, to accommodate a larger number of subcellular components into the mechanisms being represented, then one can designate a subset of *G3* grid points as indexes to separate *G3* subspaces. A *G3* subspace could represent a membrane compartment (Eason et al. 1999) or a vesicle, for example. Each *G3* subspace can be a new 2D grid of any desired size. This technique allows one to do coarse and fine spatial operations at the same time. Alternatively, an indexed *G3* subspace can be a continuous rather than discrete subspace of any desired capacity.

As stated earlier, we have shown that an EMD is both feasible and practicable for representing an *in vitro* biological system. However, that is just one use, and one small step toward our goal. The expectation is that EMD models will be used to explore *in vitro* experimental options, as well as answer what-if questions. Therefore, in designing the model and its components we do not want to restrict attention to just one cell type, e.g., Caco-2 cells. Numerous cell types are used to study drug absorption (Bohets et al. 2001). The components of our models need to be sufficiently flexible and adaptable to represent a layer of any cell type or even a layer that contains different cell types. Nor do we want to restrict attention to mimicking only transwell and similar devices. Important transport studies are done using tissue sections and lengths of whole intestine (Amidon et al. 1981). We can therefore anticipate using in silico epithelial cells that have been validated against *in vitro* data as components in a larger model representing a portion of the intestine, for example. Such flexibility and adaptability is already designed into the prototype. EMD components can be reconfigured with new components to construct and perform experiments on representations of a variety of systems.

The transport of a large number of compounds has been studied *in vitro*. Using these data, it should be possible to "train" each of the components within an EMD to recognize the physicochemical and biochemical properties of different drug-like objects. Following training, the components could, when confronted with a new object, adjust their parameters appropriately and automatically to accommodate the specific individual properties of the new compound, so that their aggregate system behavior would reasonably match the experimental data for a given, known compound. Once that is achieved for a variety of compounds, we can then dose the "educated" EMD with a new "compound", for which physicochemical and other properties are available or can be estimated. Our expectation is that we can have a measured degree of confidence that the EMD generated absorption properties will provide a reasonable prediction of expected absorption properties in the system of interest, possibly even before the compound is synthesized.

By striving to achieve these properties collectively, rather than in sequence, we will move closer to our goal. By striving to deliver the above properties, the resulting EMDs will have more in common with synthetic *in vitro* and some *in situ* and *in vivo* laboratory models, such as tissue cultures and perfused tissues, than current mathematical models.

Acknowledgements

This research was done by Yu Liu in partial fulfillment of the Ph.D. degree requirements. It was supported in part by the CDH Research Foundation (R21-CDH-00101). Early aspects of this work were presented at the 26th Annual International Conference of the IEEE EMBS (Liu et al. 2004). We thank Dr. Carolyn Cummins for data from *in vitro* Caco-2 experiments, and the members of the Biosystems Group at UCSF for helpful discussion and commentary on the manuscript, with special thanks going to Jesse Engelberg, Suman Ganguli, Pearl Johnson, Tai Ning Lam, Sunwoo Park, Glen Ropella and Jon Tang.

References

Amidon, G. E., Ho, N. F., French, A. B. and Higuchi, W. I., 1981. Predicted absorption rates with simultaneous bulk fluid flow in the intestinal tract. J Theor Biol 89, 195-210.

Andersen, M. E., 2003. Toxicokinetic modeling and its applications in chemical risk assessment. Toxicol Lett 138, 9-27.

Artursson, P. and Borchardt, R. T., 1997. Intestinal drug absorption and metabolism in cell cultures: Caco-2 and beyond. Pharm Res 14, 1655-1658.

Artursson, P., Palm, K. and Luthman, K., 2001. Caco-2 monolayers in experimental and theoretical predictions of drug transport. Adv Drug Deliv Rev 46, 27-43.

Avdeef, A., 2001. Physicochemical profiling (solubility, permeability and charge state). Curr Top Med Chem 1, 277-351.

Benet, L. Z., Cummins, C. L. and Wu, C. Y., 2004. Unmasking the dynamic interplay between efflux transporters and metabolic enzymes. Int J Pharm 277, 3-9.

Bohets, H., Annaert, P., Mannens, G., Van Beijsterveldt, L., Anciaux, K., Verboven, P., Meuldermans, W. and Lavrijsen, K., 2001. Strategies for absorption screening in drug discovery and development. Curr Top Med Chem 1, 367-383.

Camenisch, G., Alsenz, J., van de Waterbeemd, H. and Folkers, G., 1998a. Estimation of permeability by passive diffusion through Caco-2 cell monolayers using the drugs' lipophilicity and molecular weight. Eur J Pharm Sci 6, 317-324.

Camenisch, G., Folkers, G. and van de Waterbeemd, H., 1996. Review of theoretical passive drug absorption models: historical background, recent developments and limitations. Pharm Acta Helv 71, 309-327.

Camenisch, G., Folkers, G. and van de Waterbeemd, H., 1998b. Shapes of membrane permeability-lipophilicity curves: Extension of theoretical models with an aqueous pore pathway. Eur J Pharm Sci 6, 325-333.

Cummins, C. L., Mangravite, L. M. and Benet, L. Z., 2001. Characterizing the expression of CYP3A4 and efflux transporters (P-gp, MRP1, and MRP2) in CYP3A4-transfected Caco-2 cells after induction with sodium butyrate and the phorbol ester 12-O-tetradecanoylphorbol-13-acetate. Pharm Res 18, 1102-1109.

Eason, P. D. and Imperiali, B., 1999. A potent oligosaccharyl transferase inhibitor that crosses the intracellular endoplasmic reticulum membrane. Biochemistry 38, 5430-5437.

Gilbert, N. and Bankes, S., 2002. Platforms and methods for agent-based modeling. Proc Natl Acad Sci U S A 99 Suppl 3, 7197-7198.

Grass, G. M., 1997. Simulation models to predict oral drug absorption from in vitro data. Advanced Drug Delivery Reviews 23, 199-219.

Hidalgo, I. J. and Li, J., 1996. Carrier-mediated transport and efflux mechanisms in Caco-2 cells. Advanced Drug Delivery Reviews 22, 53-66.

Liu, Y. and Hunt, C. A., 2004. Representing intestinal drug transport in silico: an agent-oriented approach. The 26th Annual International Conference of the IEEE EMBS, San Francisco, CA.

Palm, K., Luthman, K., Ros, J., Grasjo, J. and Artursson, P., 1999. Effect of molecular charge on intestinal epithelial drug transport: pH-dependent transport of cationic drugs. J Pharmacol Exp Ther 291, 435-443.

Parrott, N. and Lave, T., 2002. Prediction of intestinal absorption: comparative assessment of GASTROPLUS and IDEA. Eur J Pharm Sci 17, 51-61.

Prentis, R. A., Lis, Y. and Walker, S. R., 1988. Pharmaceutical innovation by the seven UK-owned pharmaceutical companies (1964-1985). British Journal Of Clinical Pharmacology 25, 387-396.

Ropella, G. E. P., Hunt, C. A. and Nag, D. A., 2005a. Using heuristic models to bridge the gap between analytic and experimental models in biology. SpringSim'05, San Diego, CA. Available at http://biosystems.ucsf.edu/Researc/RecentPapers.html

Ropella, G. E. P., Hunt, C. A. and Sheikh-Bahaei, S., 2005b. Methodological considerations of heuristic modeling of biological systems. The 9th World Multi-Conference on Systemics, Cybernetics and Informatics, Orlando, FL. Available at http://biosystems.ucsf.edu/Researc/RecentPapers.html

Steels, L. and Brooks, R., (Eds.), 1995. The Artificial Life Route to Artificial Intelligence: Building Embodied, Situated Agents. Lawrence Earlbaum Associates, Hillsdale, NJ.

Tsuji, A. and Tamai, I., 1996. Carrier-mediated intestinal transport of drugs. Pharm Res 13, 963-977.

Walter, A. and Gutknecht, J., 1986. Permeability of small nonelectrolytes through lipid bilayer membranes. J Membr Biol 90, 207-217.

Wils, P., Warnery, A., Phung-Ba, V., Legrain, S. and Scherman, D., 1994. High lipophilicity decreases drug transport across intestinal epithelial cells. J Pharmacol Exp Ther 269, 654-658.

Xiang, T. X. and Anderson, B. D., 1993. Diffusion of ionizable solutes across planar lipid bilayer membranes: boundary-layer pH gradients and the effect of buffers. Pharm Res 10, 1654-1661.

Yu, L. X. and Amidon, G. L., 1999. A compartmental absorption and transit model for estimating oral drug absorption. Int J Pharm 186, 119-125.

Zeigler, B. P., 1990. Object-Oriented Simulation with Hierarchical, Modular Models: Intelligent Agents and Endomorphic Systems. Academic Press, San Diego, CA.